

Chemical Science

Accepted Manuscript

This article can be cited before page numbers have been issued, to do this please use: V. V. L. Heywood, T. P. J. Alford, J. J. J. Roeleveld, S. S. J. Lekanne-Deprez, A. A. Verhoofstad, J. I. van der Vlugt, M. Schnell, S. R. Domingos, A. P. Davis and T. J. Mooibroek, *Chem. Sci.*, 2020, DOI: 10.1039/D0SC01559H.



This is an Accepted Manuscript, which has been through the Royal Society of Chemistry peer review process and has been accepted for publication.

Accepted Manuscripts are published online shortly after acceptance, before technical editing, formatting and proof reading. Using this free service, authors can make their results available to the community, in citable form, before we publish the edited article. We will replace this Accepted Manuscript with the edited and formatted Advance Article as soon as it is available.

You can find more information about Accepted Manuscripts in the [Information for Authors](#).

Please note that technical editing may introduce minor changes to the text and/or graphics, which may alter content. The journal's standard [Terms & Conditions](#) and the [Ethical guidelines](#) still apply. In no event shall the Royal Society of Chemistry be held responsible for any errors or omissions in this Accepted Manuscript or any consequences arising from the use of any information it contains.

Observations of tetrel bonding between sp^3 -carbon and THF

V. L. Heywood,^[b] T. P. J. Alford,^[b] J. J. Roeleveld,^[a] S. J. Lekanne Deprez,^[a] A. Verhoofstad,^[a] J. I. van der Vlugt,^[a,c] S. R. Domingos,^[d] M. Schnell,^[d, e] A. P. Davis^[b] and T. J. Mooibroek^{*[a]}

[a] J. J. Roeleveld, S. J. Lekanne Deprez, A. Verhoofstad, Dr. J. I. van der Vlugt, Dr. T. J. Mooibroek

van 't Hoff Institute for Molecular Sciences

Universiteit van Amsterdam

Science Park 904, 1098 XH Amsterdam, The Netherlands

E-mail: t.j.mooibroek@uva.nl

[b] V. L. Heywood, T. P. J. Alford, Prof. Dr. A. P. Davis

School of Chemistry

University of Bristol

Cantock's Close, Bristol, BS8 1TS, United Kingdom

[c] Dr. J. I. van der Vlugt

Institute of Chemistry

Carl von Ossietzky University Oldenburg

Carl von Ossietzky-Straße 9-11, D-26211 Oldenburg, Germany

[d] Dr. S. R. Domingos, Prof. Dr. M. Schnell

Deutsches Elektronen-Synchrotron (DESY)

Notkestraße 85, 22607 Hamburg, Germany

[e] Prof. Dr. M. Schnell

Institut für Physikalische Chemie

Christian-Albrechts-Universität zu Kiel

Max-Eyth-Str.1, 24118 Kiel, Germany

Supporting information for this article is given via a link at the end of the document.

Keywords

sp^3 -C tetrel bonding interactions • supramolecular chemistry • crystallography • rotational spectroscopy • DFT calculations and analysis

Abstract



We report the direct observation of tetrel bonding interactions between sp^3 -carbons of the supramolecular synthon 3,3-dimethyl-tetracyanocyclopropane (**1**) and tetrahydrofuran in the gas and crystalline phase. The intermolecular contact is established via σ -holes and is driven mainly by electrostatic forces. The complex manifests distinct binding geometries when captured in the crystalline phase and in the gas phase. We elucidate these binding trends using complementary quantum chemistry calculations and find a total binding energy of $-11.2 \text{ kcal}\cdot\text{mol}^{-1}$ for the adduct. Our observations pave the way for novel strategies to engineer sp^3 -C centred non-covalent bonding schemes for supramolecular chemistry.



Introduction

Non-covalent interactions are key forces that drive phenomena such as host-guest chemistry, molecular aggregation, crystallization and protein folding.^{1, 2} In recent years, important intermolecular interactions like hydrogen and halogen bonding^{1, 3-7} have been contextualized as σ -hole interactions.⁸⁻¹⁰ A σ -hole can be seen as a Lewis acidic site along the vector of a covalent bond, the location of which coincides with the σ^* orbital of that bond. The extreme outcome of a σ -hole interaction can be the breaking and/or making of a σ bond, such as in the formation of $[I_3]^-$ from molecular I_2 and I^- .^{11, 12} A similar rationale can be applied to so-called ' π -hole interactions' involving electron deficient aromatic rings,^{13, 14} or polarized double bonds with related covalent bond-forming chemistry such as in aldol-type reactions. In principle, σ - and π -hole interactions should be available with all the non-metallic elements of the periodic table. This includes carbon;¹⁵⁻¹⁷ an element of central importance to life and ubiquitous presence in synthetic chemistry.

One might thus wonder to what extent carbon can be exploited as locus of Lewis acidity to establish 'tetrel-bonding interactions' (in analogy to halogen- and chalcogen-bonds).¹⁸ Such interactions are well-known for sp^2 -hybridized C-atoms in carbonyls¹⁹⁻²⁶ and have recently been reported for the sp -hybridized C-atoms of (coordinated) acetonitrile,²⁷ carbon monoxide²⁸ and carbon dioxide.²⁹⁻³² Non-covalent interactions with sp^3 -hybridized carbon atoms are implicated in the advent of canonical S_N2 nucleophilic displacement reactions^{12, 33-35} and can persist with methyl groups in crystal structures.³⁶⁻³⁸

However, a supramolecular synthon to predictably generate directional tetrel-bonding interactions centred on sp^3 -C has not yet been experimentally disclosed. We envisaged that 1,1,2,2-tetracyanocyclopropane (TCCP) derivatives could fulfil this role.^{39, 40} These rings are synthetically viable and contain a sterically accessible electrophilic site located roughly on the two sp^3 C-atoms in the $(NC)_2C-C(CN)_2$ fragment. This is exemplified by the molecular electrostatic potential (MEP) map of 3,3-dimethyl-TCCP (**1**) shown in Figure 1. The calculated σ -hole potential of +44 kcal·mol⁻¹ lies in-between the σ -holes of water (+55 kcal·mol⁻¹) and ammonia (+35 kcal·mol⁻¹), which are prototypical σ -hole (i.e. hydrogen bond) donors. The Lewis acidic site of **1** should thus be able to bind with an electron-rich partner such as the lone pair electron cloud on tetrahydrofuran (THF, estimated at -40 kcal·mol⁻¹).³⁹⁻⁴¹ Here we report on the verification of this hypothesis by synthesizing **1** and showing that –as anticipated– **1** binds to THF via intermolecular sp^3 -C \cdots O interactions, both in the crystalline state and in the gas phase.



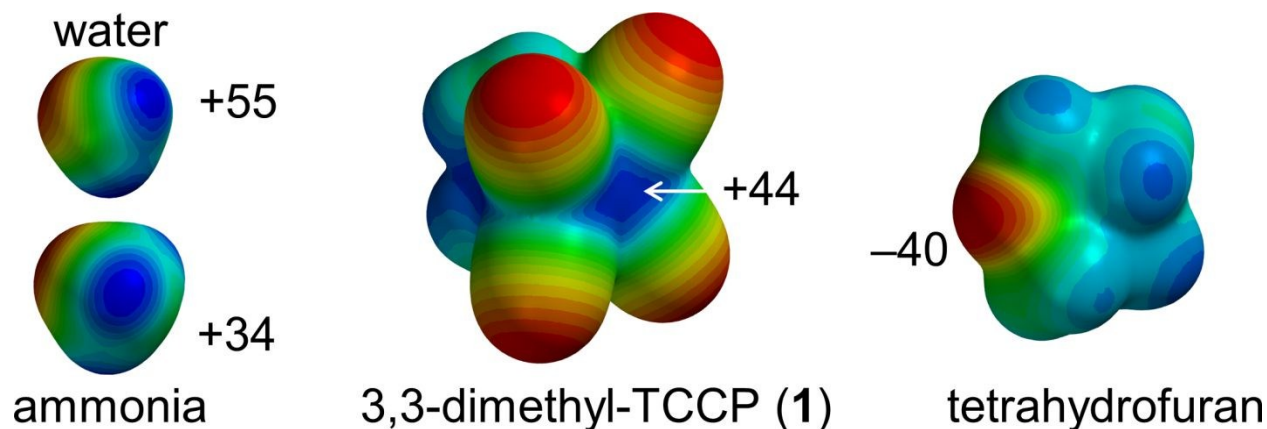
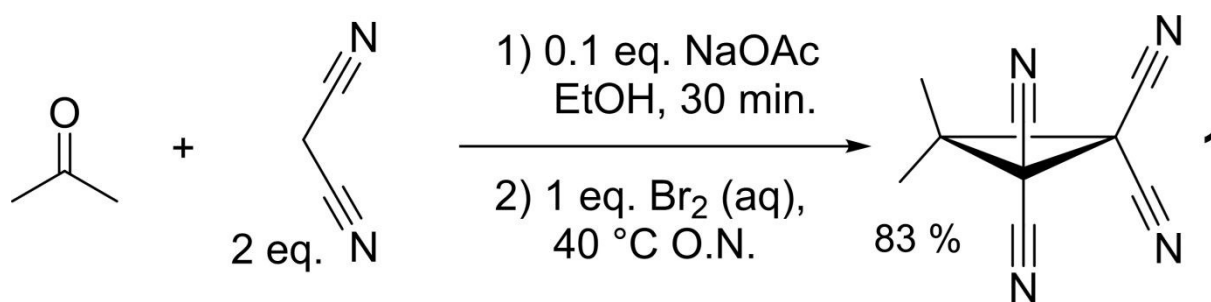


Figure 1. Molecular Electrostatic Potential maps (MEP) of water, ammonia, 3,3-dimethyl-TCCP (**1**) and tetrahydrofuran (THF) calculated at the DFT/B3LYP-D3/def2-TZVP level of theory. The MEP is colour coded from electropositive (blue) to electronegative (red), and the indicated potentials are in kcal·mol⁻¹.

Results and Discussion

Cyclopropane **1** was readily prepared in a one-pot cascade reaction from acetone, malononitrile and molecular bromine (Scheme 1). Presumably, cyclization to **1** proceeds from an intermediate formed by the nucleophilic attack of *in situ* generated [BrC(CN)₂]⁻ on the Knoevenagel condensation product of acetone and malononitrile.⁴² The yield of our procedure (83%) is higher than those reported before⁴²⁻⁴⁸ (max. 72%).⁴⁷ All literature procedures with a yield in excess of 50%^{42, 43, 45-48} (maximum 72%)⁴⁷ use a two-step approach starting from an activated malononitrile derivative^{42, 43, 45-47} and/or use electrochemical synthesis.^{47, 48}



Scheme 1. One-pot cascade synthesis of **1**.

Single crystals suitable for X-ray diffraction measurements (see ESI for details) were obtained by slow evaporation of a solution of **1** in THF. The molecular model of [1⋯THF] resulting from the diffraction study is shown in Figure 2a. All the *intramolecular* distances and angles within this



structure can be considered as normal (not shown).⁴⁹ The plane running through the O- and C-atoms of the THF molecule is roughly coplanar with the cyclopropane ring plane in **1** ($\angle_{\text{plane-plane}} = 8.2^\circ$). Interestingly, the oxygen atom of the THF molecule is directed towards C1/C3/C4 of the cyclopropane ring in **1**, with very short *intermolecular* distances, in particular $sp^3\text{-C1}\cdots\text{O1}$ of 3.007 Å ($\text{C3/C4}\cdots\text{O1} = 3.1$ Å, not shown). This is 0.213 Å within the van der Waals radii of O (1.52 Å) and C (1.70 Å) and thus consistent with a bonding interaction.^{12, 27, 39, 40, 50} Further stacking of $[\mathbf{1}\cdots\text{THF}]$ in the crystal is aided by weak $\text{N1/N2}\cdots\text{C1/C3/C4}$ interactions (max. 0.067 Å van der Waals overlap, see Figure S3).[§]

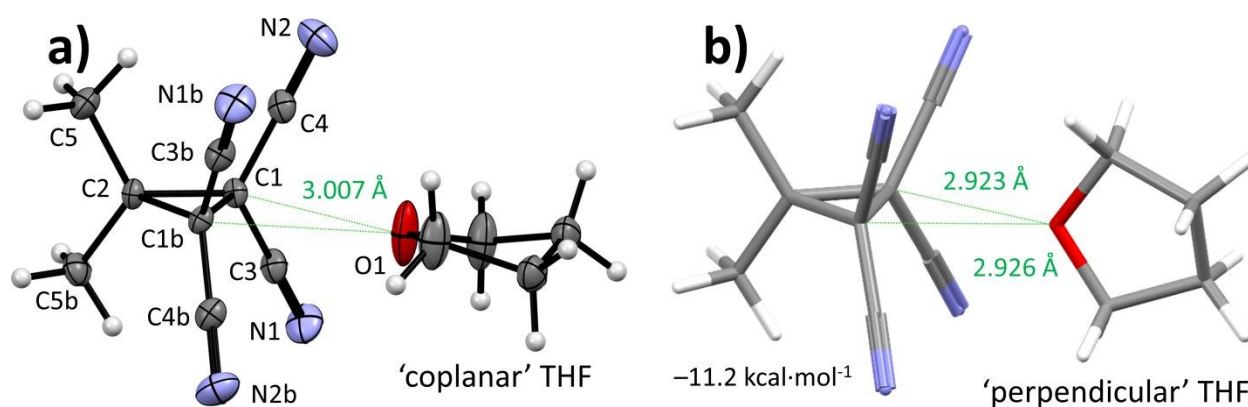


Figure 2. Left: single crystal X-ray diffraction structure of $[\mathbf{1}\cdots\text{THF}]$ with heavy atoms represented as thermal ellipsoids drawn at 50% probability and hydrogen atoms drawn as spheres with 0.15 Å radius (the unit cell was expanded along a two-fold symmetry axis running through C2 and O1). Right: Capped sticks representation of the energy minimum ($\Delta E = -11.2$ kcal·mol⁻¹) of $[\mathbf{1}\cdots\text{THF}]$ found by DFT (B3LYP-D3(BJ)/def2-TZVP) and consistent with gas phase microwave spectroscopy data. carbon = grey, nitrogen = blue, oxygen = red and hydrogen = white.

A DFT optimization at the B3LYP^{51, 52}-D3(BJ)⁵³/def2-TZVP^{54, 55} level of theory of the atomic coordinates found in the crystal structure converged at a nearly identical structure (see Figure S5). The interaction energy (ΔE) was computed to be -10.1 kcal/mol. This is much larger than interactions of dimethyl ether halogen bonded to $\text{I-C}_6\text{F}_5$ (-5.6 kcal/mol) or hydrogen bonded to water (-6.7 kcal/mol) at this same level of theory.^{37, 56} Interestingly, the $[\mathbf{1}\cdots\text{THF}]$ structure shown in Figure 2b was found to be 1.1 kcal/mol more stable, representing the true energetic minimum with $\Delta E = -11.2$ kcal/mol (see also Figure S6). The structure is similar to the crystal structure but with the THF oriented almost perpendicular to the cyclopropane plane, with $\angle_{\text{plane-plane}} = 83.8^\circ$. The distances between the THF-O and the two sp^3 (NC)₂C-C(CN)₂ atoms display up to 0.297 Å van der Waals overlap, which is 0.084 Å more than observed in the crystal structure. This



difference likely originates from the lack of any other interactions in the idealized gas phase computation *versus* various other potential weak interactions within the crystal of [1...THF].

Rotational spectroscopy is the technique to experimentally discriminate between the two relative orientations of [1...THF] (Figure 2) that are so close in energy in the gas phase calculations (1.1 kcal/mol). Thus, we conducted chirped pulse Fourier transform microwave (CP-FTMW) spectroscopy^{57, 58} to assign the geometry of [1...THF] in the gas phase (see ESI for details). Shown in Table 1 are spectroscopic parameters extracted from this experiment together with predicted values based on DFT calculations of [1...THF] with 'coplanar' or 'perpendicular' THF orientations. The experimental rotational constants (in particular B and C) provide a conclusive assignment of the [1...THF] complex in the 'perpendicular' orientation, which is also the DFT-energetic minimum (right-hand side of Figure 2).

Table 1. Rotational constants A, B, C, quartic centrifugal distortion constant D_J , and dipole moment components μ_i for [1...THF] obtained from high resolution rotational spectroscopy and compared to values predicted with DFT.^[a]

	Experiment ^[b]	DFT ^[c]	
		coplanar	perpendicular
A / MHz	632.927(43)	633.88	635.59
B / MHz	342.56932(93)	326.09	341.81
C / MHz	316.7863(10)	325.50	317.89
D_J / kHz	0.0135(35)	-	-
μ_a / D	observed	2.6	2.6
μ_b / D	not observed	0.0	0.0
μ_c / D	not observed	0.0	0.0
N^d	46	-	-
σ / kHz^[e]	22.1	-	-
$\Delta\Delta E$	-	+1.1	0
(kcal/mol)^[f]			
cj			



[a] For the purpose of structure determination of the [1 \cdots THF] adduct in the gas phase, the hyperfine structure observed in the rotational spectrum has not been fitted entirely and only centre frequencies are used for the reported fit. As such the quadrupole coupling constants for the four nitrogen nuclei are not reported at this moment. This second layer of analysis of the spectrum goes beyond the scope of this work and will be reported later in a separate manuscript. [b] The errors for the measured values are standard errors. The experimental frequency accuracy is 25 kHz. [c] The predicted rotational constants were obtained from DFT calculation at the B3LYP-D3(BJ)/def2-TZVP level of theory. 'Coplanar' and 'perpendicular' refer to the orientation of the THF ring relative to the cyclopropane ring in **1** (see also Figure 1); [d] number of lines included in the fit. [e] standard deviation of the fit.

To date we were unable to quantify tetrel bonding interactions with **1** in solution, but we did observe a very large and unusual solvent dependency of the ^1H and ^{13}C NMR resonances of **1** (detailed in Figure S7 and Table S4). For example, the methyl protons of **1**, which are γ to CN, span a range of 1.39 p.p.m. passing from benzene through toluene, acetonitrile, methanol and chloroform, to acetone. In comparison, the ethoxy methyl protons in ethyl acetate and diethyl ether vary by just 0.34 and 0.12 p.p.m., despite being closer to functional groups. These results seem to suggest strong and geometrically specific interactions between **1** and most solvent molecules. Based on these preliminary observations we anticipate that future studies will demonstrate tetrel bonding interactions with tetracyanocyclopropane derivatives in solution.

To gain more insight into the physical origins of the [1 \cdots THF] adduct, the 'perpendicular' structure was subjected to a Morokuma-Ziegler inspired energy decomposition,^{37, 59-61} an 'atoms-in-molecules'⁶², and a non-covalent interaction analysis.⁶³ The energy decomposition analysis revealed that the interaction is mainly electrostatic in origin (52.7%) followed by dispersion (30.7%) and orbital interactions (16.8%). Interestingly, orbital mixing occurred between the HOMO of THF and the LUMO of **1** ($-3.86 \text{ kcal}\cdot\text{mol}^{-1}$ stabilization) and between the HOMO-1 of THF and the HOMO of **1** ($-4.80 \text{ kcal}\cdot\text{mol}^{-1}$ stabilization, see Figure S8 for details). The 'atoms-in-molecules' analysis of [1 \cdots THF] shown in Figure 3a reveals several bond critical points (bcp's) between the N-atoms of **1** and several CH hydrogens of THF, indicating very weak hydrogen bonding interactions ($\rho \approx 0.005 \text{ a.u.}$). The densest bcp of $\rho = 0.0115 \text{ a.u.}$ is present between the THF O-atom and one of the $sp^3(\text{NC})_2\text{C}-\text{C}(\text{CN})_2$ atoms (highlighted in yellow).^{§§} In line with these results, the NCI plot shown in Figure 3b clearly reveals that there are two $sp^3\text{-C}\cdots\text{O}$ interactions that are mainly electrostatic in origin (blue), and that the $\text{C}-\text{H}\cdots\text{N}$ interactions are mainly dispersive (yellow/green).



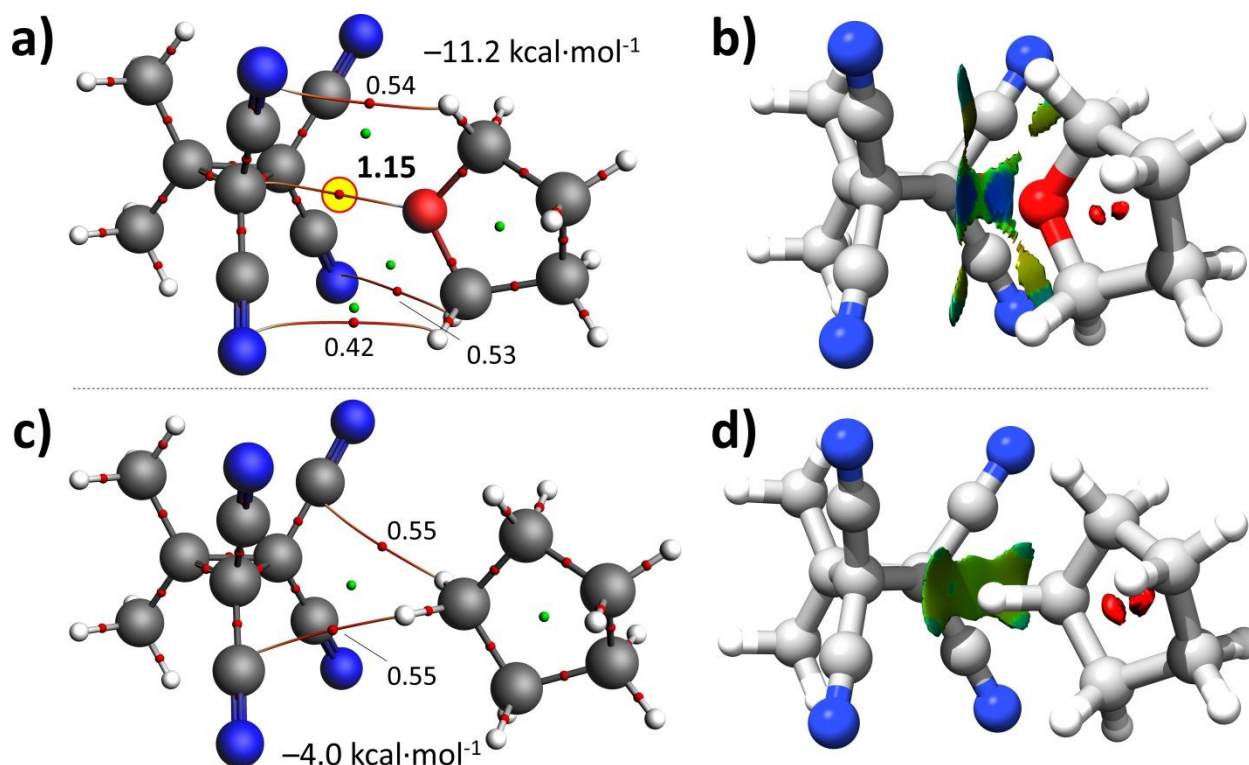


Figure 3. Geometry optimized structures (B3LYP-D3/def2-TZVP) and ‘atoms-in-molecules’ analysis of [1...THF] (a, see also Figure 2) and [1...cyclopentane] (c, obtained after *in silico* O \rightarrow CH₂ mutation and optimization). The bond densities of the intermolecular bond critical points are represented by small red spheres (ρ in a.u. $\times 100$). b) and d) show a non-covalent interactions (NCI) analysis using NCIPLOT. Isolevel = 0.3 and regions in blue are mainly electrostatic interactions, in green are van der Waals dispersive forces and repulsions are in red.

For comparison purposes, a cyclopentane adduct was calculated after *in silico* O \rightarrow CH₂ mutation and geometry optimization of structure [1...THF]. This resulted in the structurally similar [1...cyclopentane] adduct shown in Figure 3c (see also Figure S9). The ‘atoms-in-molecules’ analysis of this adduct reveals only two C–H...C \equiv N bcp’s ($\rho \approx 0.0055 \text{ a.u.}$). The adduct is also much less stable with $\Delta E = -4.0 \text{ kcal/mol}$, which is mainly driven by dispersion (59.4%) followed by electrostatic interactions (22.2%). The NCI analysis of this adduct depicted in Figure 3d clearly shows that this adduct is only held by dispersive C–H...N interactions (green).

Summary and concluding remarks

In summary, it was shown that **1** can form [1...THF] complexes in the crystalline state and in the gas phase with a calculated interaction energy of up to -11.2 kcal/mol . These complexes are held



together by strong polar interactions between the *de facto* Lewis acidic site in between the sp^3 -hybridized C-atoms of **1** and the Lewis basic THF-O. These results demonstrate that tetrel-bonding interactions with sp^3 -carbon centres can indeed be used to engineer supramolecular complexes, thus paving the way for their exploration in other molecular disciplines, e. g. supramolecular chemistry, crystal engineering and medicine.

Conflicts of interest

The authors declare no conflict of interest.

Acknowledgements

TJM thanks NWO (VIDI project 723.015.006) and the EPSRC (EP/I028501/1) for funding. MS acknowledges financial support by the Deutsche Forschungsgemeinschaft in the context of the priority program SPP1807 (SCHN1280/4-2).

Notes and references

1. P. J. Cragg, *Supramolecular Chemistry: From Biological Inspiration to Biomedical Applications*, Springer, Dordrecht, 1 edn., 2010.
2. A. Bauza, T. J. Mooibroek and A. Frontera, *ChemPhysChem*, 2015, **16**, 2496-2517.
3. H. J. Schneider, *Supramolecular Systems in Biomedical Fields*, RSC Publishing, Cambridge, UK, 1 edn., 2013.
4. T. Steiner, *Angew. Chem.-Int. Edit.*, 2002, **41**, 48-76.
5. P. Metrangolo, H. Neukirch, T. Pilati and G. Resnati, *Acc. Chem. Res.*, 2005, **38**, 386-395.
6. *Hydrogen Bonding: New Insights*, Springer, Heidelberg, 2006.
7. M. R. Scholfield, C. M. Vander Zanden, M. Carter and P. S. Ho, *Protein Sci.*, 2013, **22**, 139-152.
8. P. Politzer, J. S. Murray and P. Lane, *Int. J. Quantum Chem.*, 2007, **107**, 3046-3052.
9. S. J. Grabowski, *Phys. Chem. Chem. Phys.*, 2013, **15**, 7249-7259.
10. S. Scheiner, *Acc. Chem. Res.*, 2013, **46**, 280-288.
11. R. H. Crabtree, *Chem. Soc. Rev.*, 2017, **46**, 1720-1729.
12. A. Bauza, T. J. Mooibroek and A. Frontera, *Chem. Rec.*, 2016, **16**, 473-487.
13. C. A. Hunter and J. K. M. Sanders, *J. Am. Chem. Soc.*, 1990, **112**, 5525-5534.
14. B. L. Schottel, H. T. Chifotides and K. R. Dunbar, *Chem. Soc. Rev.*, 2008, **37**, 68-83.
15. S. J. Grabowski, *Chem.-Eur. J.*, 2013, **19**, 14600-14611.
16. J. S. Murray, P. Lane and P. Politzer, *J. Mol. Model.*, 2009, **15**, 723-729.
17. A. Bauza, T. J. Mooibroek and A. Frontera, *ChemPhysChem*, 2015, **16**, 2496-2517.
18. C. B. Aakeroy, D. L. Bryce, G. Desiraju, A. Frontera, A. C. Legon, F. Nicotra, K. Rissanen, S. Scheiner, G. Terraneo, P. Metrangolo and G. Resnati, *Pure Appl. Chem.*, 2019, **91**, 1889-1892.

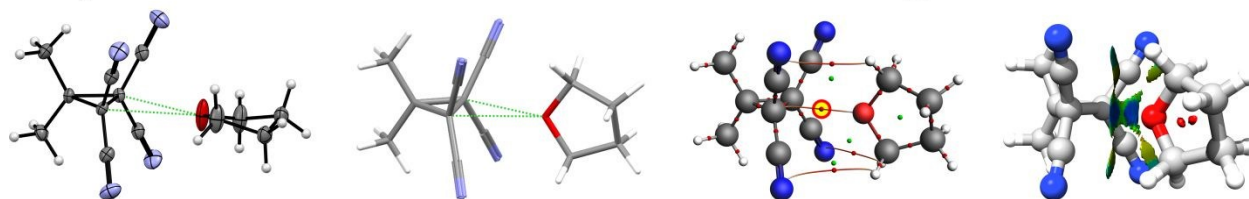


19. P. Murrayrust, H. B. Burgi and J. D. Dunitz, *J. Am. Chem. Soc.*, 1975, **97**, 921-922.
20. H. B. Burgi, *Angew. Chem. Int. Ed.*, 1975, **14**, 460-473.
21. M. Harder, B. Kuhn and F. Diederich, *ChemMedChem*, 2013, **8**, 397-404.
22. G. J. Bartlett, A. Choudhary, R. T. Raines and D. N. Woolfson, *Nat. Chem. Biol.*, 2010, **6**, 615-620.
23. P. H. Maccallum, R. Poet and E. J. Milnerwhite, *J. Mol. Biol.*, 1995, **248**, 374-384.
24. A. Choudhary, D. Gandla, G. R. Krow and R. T. Raines, *J. Am. Chem. Soc.*, 2009, **131**, 7244-7246.
25. R. W. Newberry, G. J. Bartlett, B. VanVeller, D. N. Woolfson and R. T. Raines, *Protein Sci.*, 2014, **23**, 284-288.
26. E. C. Vik, P. Li, P. J. Pellechia and K. D. Shimizu, *J. Am. Chem. Soc.*, 2019, **141**, 16579-16583.
27. A. R. van der Werve, Y. R. van Dijk and T. J. Mooibroek, *Chem. Commun.*, 2018, **54**, 10742-10745.
28. M. T. Doppert, H. van Overeem and T. J. Mooibroek, *Chem. Commun.*, 2018, **54**, 12049-12052.
29. Y. P. Zeng, S. W. Sharpe, S. K. Shin, C. Wittig and R. A. Beaudet, *J. Chem. Phys.*, 1992, **97**, 5392-5402.
30. A. C. Legon, *Phys. Chem. Chem. Phys.*, 2017, **19**, 14884-14896.
31. S. Gao, D. A. Obenchain, J. C. Lei, G. Feng, S. Herbers, Q. Gou and J. U. Grabow, *Phys. Chem. Chem. Phys.*, 2019, **21**, 7016-7020.
32. M. Juanes, R. T. Saragi, W. Caminati and A. Lesarri, *Chem.-Eur. J.*, 2019, **25**, 11402-11411.
33. J. Langer, S. Matejcik and E. Illenberger, *Phys. Chem. Chem. Phys.*, 2000, **2**, 1001-1005.
34. J. Mikosch, S. Trippel, C. Eichhorn, R. Otto, U. Lourderaj, J. X. Zhang, W. L. Hase, M. Weidemuller and R. Wester, *Science*, 2008, **319**, 183-186.
35. S. Pierrefixe, J. Poater, C. Im and F. M. Bickelhaupt, *Chem.-Eur. J.*, 2008, **14**, 6901-6911.
36. V. R. Mundlapati, D. K. Sahoo, S. Bhaumik, S. Jena, A. Chandrakar and H. S. Biswal, *Angew. Chem.-Int. Edit.*, 2018, **57**, 16496-16500.
37. T. J. Mooibroek, *Molecules*, 2019, **24**, At. Nr: 3370.
38. J. Dutta, D. Kumar Sahoo, S. Jena, K. D. Tulsiyan and H. S. Biswal, *Phys. Chem. Chem. Phys.*, 2020, DOI: 10.1039/D1030CP00330A.
39. A. Bauza, A. Frontera and T. J. Mooibroek, *Phys. Chem. Chem. Phys.*, 2016, **18**, 1693-1698.
40. A. Bauza, T. J. Mooibroek and A. Frontera, *Chem.-Eur. J.*, 2014, **20**, 10245-10248.
41. A. Bauza, T. J. Mooibroek and A. Frontera, *Phys. Chem. Chem. Phys.*, 2014, **16**, 19192-19197.
42. A. N. Vereshchagin, M. N. Elinson, N. O. Stepanov and G. I. Nikishin, *Mendeleev Commun.*, 2009, **19**, 324-325.
43. R. Huisgen and G. Mloston, *Heterocycles*, 1990, **30**, 737-740.
44. K. Kouno and Y. Ueda, *Chem. Pharm. Bull.*, 1985, **33**, 3998-4001.
45. H. Hart and Y. C. Kim, *J. Org. Chem.*, 1966, **31**, 2784-2789.
46. R. Huisgen, G. Mloston and E. Langhals, *Helv. Chim. Acta*, 2001, **84**, 1805-1820.
47. M. N. Elinson, S. K. Feducovich, T. L. Lizunova and G. I. Nikishin, *Tetrahedron*, 2000, **56**, 3063-3069.
48. G. I. Nikishin, M. N. Elinson, T. L. Lizunova and B. I. Ugrak, *Tetrahedron Lett.*, 1991, **32**, 2655-2656.
49. F. H. Allen, O. Kennard, D. G. Watson, L. Brammer, A. G. Orpen and R. Taylor, *J. Chem. Soc.-Perkin Trans. 2*, 1987, DOI: 10.1039/p2987000000s1, S1-S19.
50. A. Bondi, *J. Phys. Chem.*, 1964, **68**, 441-452.
51. A. D. Becke, *Phys. Rev. A*, 1988, **38**, 3098-3100.
52. C. T. Lee, W. T. Yang and R. G. Parr, *Phys. Rev. B*, 1988, **37**, 785-789.
53. S. Grimme, J. Antony, S. Ehrlich and H. Krieg, *J. Chem. Phys.*, 2010, **132**, Art. Nr: 154104.
54. F. Weigend and R. Ahlrichs, *Phys. Chem. Chem. Phys.*, 2005, **7**, 3297-3305.
55. F. Weigend, *Phys. Chem. Chem. Phys.*, 2006, **8**, 1057-1065.
56. J. M. Hoffmann, A. K. Sadhoe and T. J. Mooibroek, *Synthesis*, 2020, **52**, 521-528.
57. G. G. Brown, B. C. Dian, K. O. Douglass, S. M. Geyer, S. T. Shipman and B. H. Pate, *Rev. Sci. Instrum.*, 2008, **79**, Art Nr: 053103.



58. S. R. Domingos, K. Martin, N. Avarvari and M. Schnell, *Angew. Chem.-Int. Edit.*, 2019, **58**, 11257-11261.
59. G. te Velde, F. M. Bickelhaupt, E. J. Baerends, C. F. Guerra, S. J. A. van Gisbergen, J. G. Snijders and T. Ziegler, *J. Comput. Chem.*, 2001, **22**, 931-967.
60. F. M. Bickelhaupt and E. J. Baerends, in *Reviews in Computational Chemistry, Vol 15*, eds. K. B. Lipkowitz and D. B. Boyd, Wiley-Vch, Inc, New York, 2000, vol. 15, pp. 1-86.
61. S. C. C. van der Lubbe and C. F. Guerra, *Chem. Asian J.*, 2019, **14**, 2760-2769.
62. R. F. W. Bader, *Acc. Chem. Res.*, 1985, **18**, 9-15.
63. J. Contreras-Garcia, E. R. Johnson, S. Keinan, R. Chaudret, J. P. Piquemal, D. N. Beratan and W. T. Yang, *J. Chem. Theory Comput.*, 2011, **7**, 625-632.
64. G. R. Fulmer, A. J. M. Miller, N. H. Sherden, H. E. Gottlieb, A. Nudelman, B. M. Stoltz, J. E. Bercaw and K. I. Goldberg, *Organometallics*, 2010, **29**, 2176-2179.

sp^3 -C centered tetrel bonding *in action*



Supramolecular adducts were generated using sp^3 -C centred tetrel bonding interactions, both in the crystalline state and in the gas phase. Calculations using density functional theory revealed interaction energies up to $-11.2 \text{ kcal}\cdot\text{mol}^{-1}$ and showed that these adducts are held together mainly by electrostatics.

